

**A UV Solar-Blind Nonlinear Optical Crystal with Confined  $\pi$ -Conjugated Groups**

Xianyu Song,<sup>a,b</sup> Zhipeng Du,<sup>a,b</sup> Belal Ahmed,<sup>d</sup> Yanqiang Li,<sup>b</sup> Yang Zhou,<sup>b</sup> Yipeng Song,<sup>b</sup> Weiqi Huang,<sup>b</sup> Jieyu Zheng,<sup>b</sup> Junhua Luo,<sup>b,c</sup> and Sangen Zhao<sup>b,c,\*</sup>

<sup>a</sup>College of Chemistry, Fuzhou University, Fuzhou 350116, China

<sup>b</sup>State Key Laboratory of Structural Chemistry, Fujian Institute of Research on the Structure of Matter, Chinese Academy of Sciences, Fuzhou 350002, China

<sup>c</sup>Fujian Science & Technology Innovation Laboratory for Optoelectronic Information of China, Fuzhou 350108, China

<sup>d</sup>Department of Chemistry, Shahjalal University of Science and Technology, Sylhet 3114, Bangladesh.

## CONTENTS

Single-Crystal Structure Determination.....	1
Powder X-Ray Diffraction.....	1
Elemental Analysis and Scanning Electron Microscope Mapping.....	2
UV-Vis-NIR Transmission Spectroscopy.....	2
Thermal Stability.....	2
SHG Measurements.....	2
Birefringence Tests.....	3
Theoretical Calculations.....	3
Figure S1. Single-crystal of RPNCO obtained after recrystallization .....	5
Figure S2. (a) The original single crystals of RPNCO (b) Corresponding single crystals of RPNCO were exposed to the air at room temperature for two weeks.....	5
Figure S3. The experimental powder XRD patterns of RPNCO crystal exposed to the air at room temperature for more than two weeks, and the simulated powder XRD pattern of RPNCO.....	6
Figure S4. Energy dispersive X-ray (EDX) analysis of RPNCO.....	6
Figure S5. TG and DTA diagrams of RPNCO.....	7
Figure S6 The thickness of the selected RPNCO single-crystal used for the birefringence measurement.....	7
Figure S7 Electronic band structure of RPNCO calculated by GGA.....	8
Figure S8 Electronic band structure of RPNCO calculated by HSE06.....	8
Table S1. Crystallographic data and structural refinement for RPNCO.....	9
Table S2. Atomic coordinates ( $\times 10^4$ ) and equivalent isotropic displacement parameters ( $\text{\AA}^2 \times 10^3$ ) for RPNCO.....	10
Table S3. Anisotropic displacement parameters ( $\text{\AA}^2$ ) for RPNCO.....	11
Table S4. Selected bond distances ( $\text{\AA}$ ) for RPNCO.....	12
Table S5. Selected bond angles ( $^\circ$ ) for RPNCO.....	13
Table S6. Selected hydrogen-bond interactions of RPNCO.....	14
References .....	14

## **Single-Crystal Structure Determination.**

A high-quality colorless crystal of RPNCO was selected using an optical microscope for single-crystal X-ray diffraction (XRD) analysis. The diffraction data were collected by using graphite-monochromatized Cu K $\alpha$  radiation ( $\lambda = 1.5418 \text{ \AA}$ ) at 200(2) K on an Agilent SuperNova diffractometer with an Atlas detector. The collection of the intensity data, cell refinement, and data reduction was carried out with the CrysAlisPro software (version 1.171.41.116a). Using Olex2,<sup>1</sup> the structure was solved with the SHELXS<sup>2</sup> structure solution program using Direct Methods and refined with the SHELXL<sup>3</sup> refinement package using Least Squares minimisation. Final refinements include anisotropic displacement parameters. Both structures were verified by the ADDSYM algorithm from the program PLATON,<sup>4</sup> and no higher symmetry was found. Details of crystal parameters, data collection, and structure refinement were summarized in Table S1. The atomic coordinates and equivalent isotropic displacement parameters were listed in Table S2. The anisotropic displacement parameters were listed in Table S3. Selected bond lengths and bond angles were presented in Table S4 and Table S5. Selected hydrogen-bond interactions were presented in Table S6.

## **Powder X-Ray Diffraction.**

Powder X-ray diffraction (PXRD) measurement for the sample of RPNCO was carried out with a Miniflex 600 diffractometer equipped with an incident beam monochromator set of Cu K $\alpha$  radiation ( $\lambda = 1.5418 \text{ \AA}$ ), and the 2 $\theta$  range of 5-70°, with a scan step width of 0.02° and a scanning rate of 4° min<sup>-1</sup>.

### **Elemental Analysis and Scanning Electron Microscope Mapping.**

The elemental analysis was performed on the Vario MICRO cube Elementar. In addition, the scanning electron microscope (SEM) elemental mapping on the RPNCO single crystal was collected on a field emission SEM (Hitachi SU8010).

### **UV-Vis-NIR Transmission Spectroscopy.**

UV-Vis-NIR transmission spectral data were recorded at room temperature with a PerkinElmer Lamda-950 UV-Vis-NIR spectrophotometer. The scanned wavelength range was 190 nm to 800 nm using transparent bulk crystals obtained from natural growth.

### **Thermal Stability.**

The thermal stability was investigated by the differential thermal analysis (DTA) on a simultaneous NETZSCH STA 449C thermal analyzer in an atmosphere of flowing N<sub>2</sub>. About 11.43 mg RPNCO powders were placed into an Al<sub>2</sub>O<sub>3</sub> crucible, and heated at a rate of 15 K·min<sup>-1</sup> from room temperature to 1000 K (Figure S4).

### **SHG Measurements.**

The second harmonic generation (SHG) measurements were performed on a Q-switched Nd: YAG laser at the wavelength of 1064 nm. Polycrystalline samples of RPNCO were ground and sieved into the following particle size ranges: 53-61 µm, 61-74 µm, 74-124 µm, 124-178 µm, 178-250 µm, and 250-297 µm. All samples were pressed between glass slides and secured with tape in 1-mm thick aluminum holders containing an 8-mm diameter hole. They were then placed into a light-tight box and irradiated with the laser. The intensity of the frequency-doubled output emitted from

the samples was collected by a photomultiplier tube. Crystalline KH<sub>2</sub>PO<sub>4</sub> (KDP) samples were also ground, sieved into the same particle size ranges, and used as references.

### Birefringence Tests.

The birefringence of RPNCO was characterized by the polarized method under the polarized microscope (Nikon ECLIPSE LV100N POL) equipped with a Berek compensator. The wavelength of the light source was  $\lambda = 550$  nm. The relative error is small enough because of the clear boundary lines of the first-, second- and third-order interference color. In order to improve the accuracy of the birefringence, small and transparent RPNCO crystals were chosen. The tested crystal planes were determined by single-crystal XRD diffraction. The formula for calculating the birefringence is listed below:<sup>5, 6</sup>

$$R = | n_e - n_o | \times d = \Delta n \times d$$

Here, R represents the optical path difference,  $\Delta n$  is the birefringence, and  $d$  denotes the thickness of the tested crystal.

### Theoretical Calculations.

The first-principles calculations were carried out with the CASTEP software,<sup>7</sup> a plane-wave pseudopotential package<sup>8</sup> on the basis of the density functional theory (DFT).<sup>9</sup> The exchange-correlation energy was described by the generalized gradient approximation (GGA) scheme of the Perdew-Burke-Ernzerhof (PBE) functional, as implemented in the CASTEP code.<sup>10</sup> Norm-conserving pseudopotentials were employed to simulate the ion-electron interactions for each atomic specie with following valence configurations: H 1s<sup>1</sup>, C 2s<sup>2</sup> 2p<sup>2</sup>, N 2s<sup>2</sup> 2p<sup>3</sup>, O 2s<sup>2</sup> 2p<sup>4</sup>, P 3s<sup>2</sup> 3p<sup>3</sup>, Rb 4s<sup>2</sup> 4p<sup>6</sup> 5s<sup>1</sup>.<sup>11</sup> A cutoff energy of 900 eV and the Monkhorst-Pack<sup>12</sup> k-point meshes ( $5 \times 1 \times 5$ ) spacing about 0.03 Å<sup>-1</sup> in the Brillouin zone were chosen for the calculation.

Considering that GGA-PBE usually severely underestimates the band gap, the HSE06 functional<sup>13</sup> was employed to further calculate the band gap for RPNCO. Herein, all calculations were performed without the scissors operator.

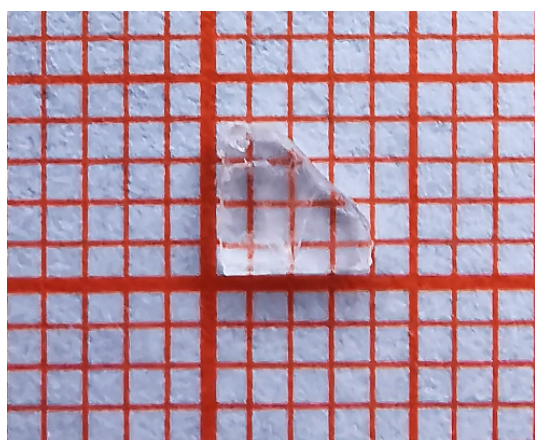


**Figure S1.** Single-crystal of RPNCO obtained after recrystallization

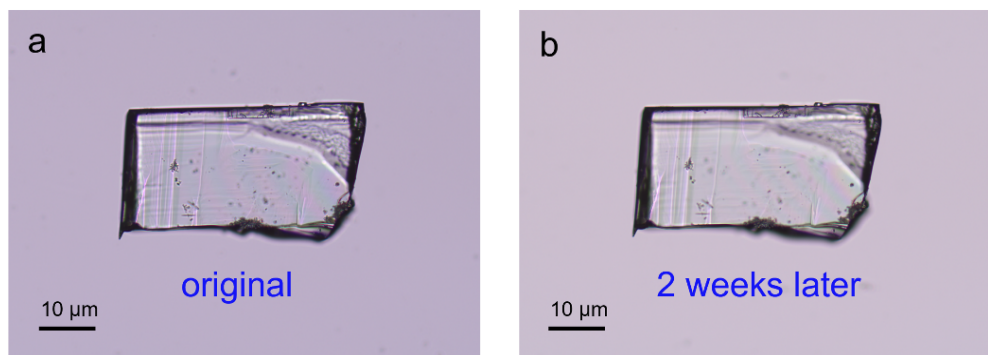


**Figure S2.** (a) The original single crystals of RPNCO (b) Corresponding single crystals

of RPNCO were exposed to the air at room temperature for two weeks.

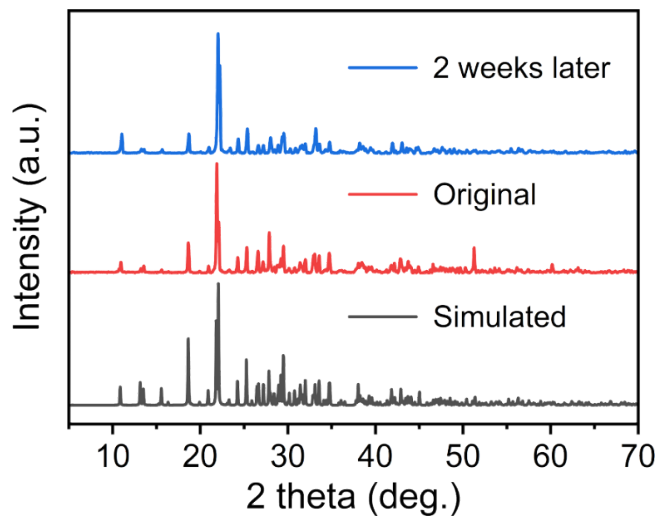


**Figure S3.** The experimental powder XRD patterns of RPNCO crystal exposed to the air at room temperature for more than two weeks, and the simulated powder XRD pattern of RPNCO.

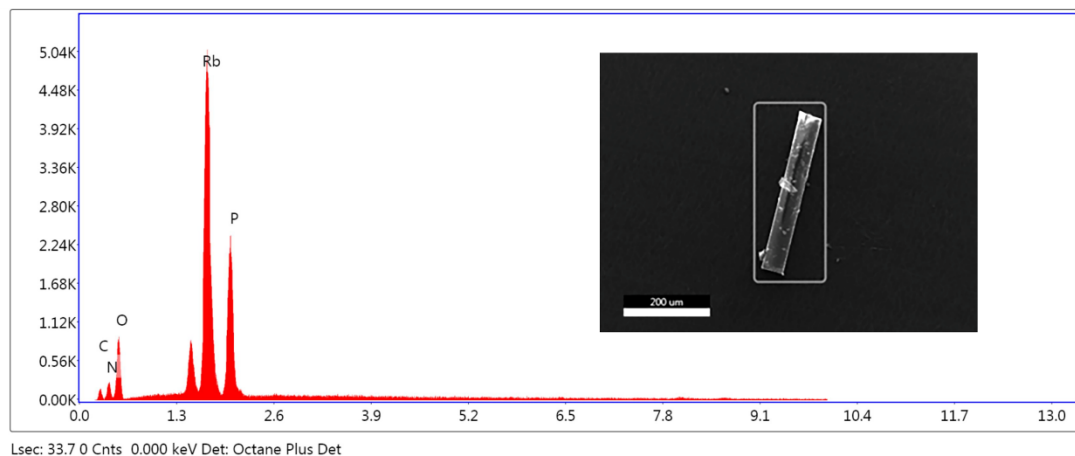


**Figure S4.** Energy dispersive X-ray (EDX) analysis of RPNCO.

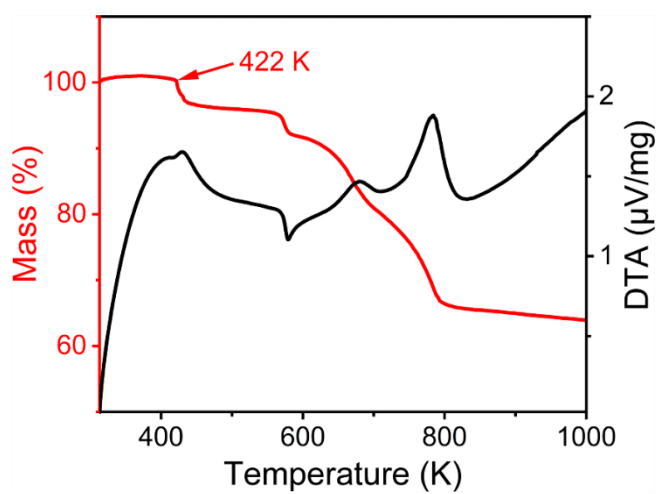


**Figure S5.** TG and DTA diagrams of RPNCO.



**Figure S6** The thickness of the selected RPNCO single-crystal used for the birefringence measurement.

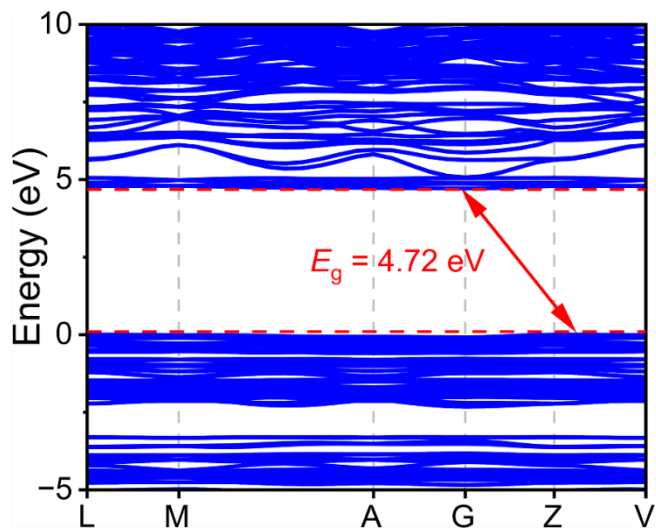


**Figure S7** Electronic band structure of RPNCO calculated by GGA.

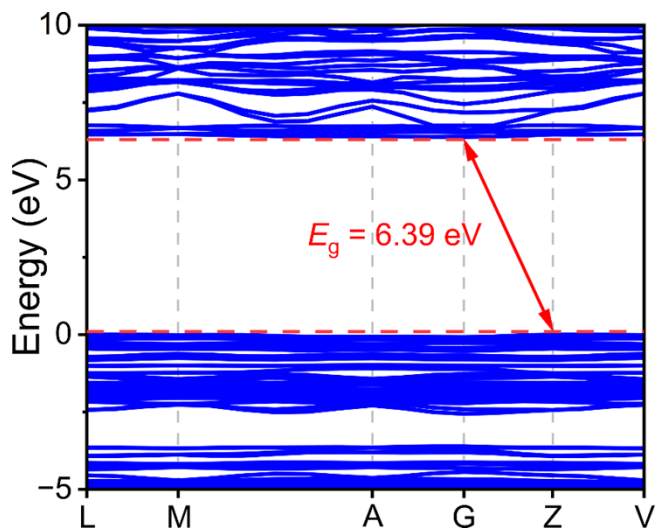


**Figure S8** Electronic band structure of RPNCO calculated by HSE06.

**Table S1.** Crystallographic data and structural refinement for RPNCO.

Empirical formula	C <sub>4</sub> H <sub>8</sub> N <sub>6</sub> O <sub>9</sub> P <sub>2</sub> Rb <sub>2</sub>
Formula weight	517.04
Temperature/K	200.15
Crystal system	monoclinic
Space group	Cc
a/Å	6.6882(2)
b/Å	32.5229(10)
c/Å	6.8991(2)
α/°	90
β/°	94.173(2)
γ/°	90
Volume/Å <sup>3</sup>	1496.71(8)
Z	4
ρ(g/cm <sup>3</sup> )	2.295
μ/mm <sup>-1</sup>	11.091
F(000)	1000
Radiation	Cu K $\alpha$ ( $\lambda = 1.54184$ )
2θ range for data collection/°	10.882 to 145.258
Index ranges	-8 ≤ h ≤ 6, -38 ≤ k ≤ 36, -8 ≤ l ≤ 5
Reflections collected	3772
Independent reflections	1947 ( $R_{\text{int}} = 0.0201$ , $R_{\text{sigma}} = 0.0210$ )
Data/restraints/parameters	1947/3/214
Goodness-of-fit on F <sup>2</sup>	1.005
Final R indexes (I ≥ 2σ(I)) <sup>[a]</sup>	$R_1 = 0.0293$ , $wR_2 = 0.0745$
Final R indexes (all data) <sup>[a]</sup>	$R_1 = 0.0295$ , $wR_2 = 0.0747$
Largest diff. peak/hole (e Å <sup>-3</sup> )	0.55/-0.44
Flack parameter	-0.04(2)

[a]  $R_1 = \sum ||F_o| - |F_c|| / \sum |F_o|$  and  $wR_2 = [\sum w(F_o^2 - F_c^2)^2 / \sum wF_o^4]^{1/2}$  for  $F_o^2 > 2\sigma(F_o^2)$ .

**Table S2.** Atomic coordinates ( $\times 10^4$ ) and equivalent isotropic displacement parameters ( $\text{\AA}^2 \times 10^3$ ) for RPNCO.

Atom	x	y	z	$U(\text{eq})^{[\text{a}]}$
Rb1	743.7(7)	3016.6(2)	2527.7(7)	19.54(19)
Rb2	9492.4(9)	4419.7(2)	10126.2(9)	28.7(2)
P1	4151(2)	4412.0(4)	6609.5(19)	13.2(3)
P2	3649(2)	3035.4(4)	7786(2)	11.2(3)
C1	5574(8)	4689.2(18)	3255(8)	15.2(11)
C2	4076(8)	3996.2(18)	3189(8)	15.3(11)
C3	7158(8)	2838.8(19)	6209(8)	15.9(12)
C4	7319(9)	3368.3(18)	8812(8)	14.8(11)
N1	5347(8)	4729.9(15)	5163(7)	16.0(9)
N2	4768(8)	4342.2(15)	2315(7)	16.3(10)
N3	4004(8)	3996.5(15)	5129(7)	19.6(10)
N4	5197(7)	2785.8(16)	6378(7)	17.6(10)
N5	8096(7)	3151.3(17)	7303(7)	17.6(10)
N6	5354(7)	3330.0(14)	9030(7)	16.6(10)
O1	6441(6)	4944.8(13)	2292(6)	18.3(8)
O2	3544(7)	3696.3(14)	2177(7)	27.1(10)
O3	2072(7)	4557.3(14)	6889(6)	24.2(10)
O4	5443(7)	4327.7(14)	8387(6)	23.3(9)
O5	8140(6)	2629.9(14)	5141(7)	24.0(10)
O6	8448(6)	3578.5(14)	9883(7)	23.5(9)
O7	2738(6)	2740.7(13)	9122(6)	16.7(8)
O8	2189(6)	3291.4(13)	6569(6)	17.6(8)
O9	9261(9)	4094(2)	14294(10)	57.7(18)

[a]  $U_{\text{eq}}$  is defined as one-third of the trace of the orthogonalized  $U_{ij}$  tensor.

**Table S3.** Anisotropic displacement parameters ( $\text{\AA}^2$ ) for RPNCO.

Atom	U11	U22	U33	U23	U13	U12
Rb1	18.8(3)	21.8(3)	18.2(3)	1.8(2)	2.91(19)	-1.5(2)
Rb2	24.6(3)	30.7(4)	31.8(4)	-11.6(3)	8.2(2)	-10.1(2)
P1	17.2(8)	12.7(7)	10.2(7)	0.4(5)	3.6(6)	-0.1(5)
P2	9.2(6)	11.4(7)	13.3(7)	-0.4(5)	2.5(5)	-0.8(5)
C1	14(3)	17(3)	15(2)	-1(2)	2(2)	0(2)
C2	16(3)	16(3)	15(3)	-3(2)	3(2)	-5(2)
C3	9(3)	20(3)	19(3)	2(2)	2(2)	5(2)
C4	15(2)	12(3)	17(3)	3(2)	-4(2)	-2(2)
N1	22(2)	11(2)	14(2)	-0.9(17)	0.2(19)	-3.4(19)
N2	19(2)	16(3)	15(2)	-1.6(18)	5.8(18)	-5(2)
N3	27(3)	15(3)	18(2)	0.6(19)	5(2)	-5(2)
N4	16(2)	18(3)	20(2)	-9.5(17)	3.9(19)	-4.0(18)
N5	9(2)	20(3)	24(3)	-2(2)	3.7(19)	-1(2)
N6	15(2)	13(3)	22(3)	-9.8(19)	1.4(19)	0.5(19)
O1	21(2)	16(2)	18.5(19)	2.2(15)	3.5(15)	-5.7(17)
O2	35(3)	23(2)	24(2)	10.1(17)	10.3(19)	12.5(19)
O3	25(2)	23(2)	26(2)	9.9(18)	12.1(19)	9.9(19)
O4	28(2)	27(2)	15(2)	2.6(17)	-3.8(18)	-2.6(19)
O5	19(2)	26(2)	28(2)	-8.0(19)	10.5(18)	-0.4(18)
O6	20(2)	23(2)	27(2)	-7.2(17)	-4.9(16)	-4.5(18)
O7	16(2)	18(2)	16.6(19)	1.9(16)	3.9(15)	-0.7(16)
O8	13.6(18)	19(2)	20.0(19)	3.6(16)	1.7(15)	-1.3(15)
O9	38(3)	75(5)	58(4)	-4(3)	-6(3)	2(3)

**Table S4.** Selected bond distances ( $\text{\AA}$ ) for RPNCO.

Selected bonds	Length( $\text{\AA}$ )	Selected bonds	Length( $\text{\AA}$ )
Rb1-O7 <sup>[1]</sup>	2.974(4)	P1-O4	1.474(4)
Rb1-O7 <sup>[2]</sup>	2.926(4)	P1-O3	1.494(5)
Rb1-O8	3.019(4)	P1-N3	1.693(5)
Rb1-O5 <sup>[3]</sup>	3.122(5)	P1-N1	1.680(5)
Rb1-O5 <sup>[4]</sup>	2.885(4)	O1-C1	1.234(7)
Rb1-O6 <sup>[5]</sup>	2.936(5)	O5-C3	1.227(7)
Rb1-O2	2.919(5)	O6-C4	1.225(7)
Rb2-O1 <sup>[6]</sup>	2.814(4)	O2-C2	1.236(7)
Rb2-O1 <sup>[7]</sup>	3.124(4)	N3-C2	1.343(8)
Rb2-O6	2.825(5)	N4-C3	1.337(7)
Rb2-O4	2.897(4)	N1-C1	1.343(8)
Rb2-O3 <sup>[8]</sup>	2.954(4)	N2-C1	1.390(7)
Rb2-O9	3.079(7)	N2-C2	1.373(7)
P2-O7	1.490(4)	N6-C4	1.340(8)
P2-O8	1.494(4)	C4-N5	1.389(8)
P2-N4	1.680(5)	C3-N5	1.388(8)
P2-N6	1.677(5)		

<sup>[1]</sup>+X,1/2-Y,-1/2+Z; <sup>[2]</sup>+X,+Y,-1+Z; <sup>[3]</sup>-1+X,1/2-Y,-1/2+Z; <sup>[4]</sup>-1+X,+Y,+Z; <sup>[5]</sup>-1+X,+Y,-1+Z;  
<sup>[6]</sup>1/2+X,1-Y,1+Z; <sup>[7]</sup>+X,+Y,1+Z; <sup>[8]</sup>1+X,+Y,+Z

**Table S5.** Selected bond angles ( $^{\circ}$ ) for RPNCO.

Selected bond angles	Angle( $^{\circ}$ )	Selected bond angles	Angle( $^{\circ}$ )
O7-P2-O8	115.2(2)	C2-N2-C1	126.3(5)
O7-P2-N4	110.1(2)	C4-N6-P2	129.2(4)
O7-P2-N6	110.1(2)	O1-C1-N1	123.5(5)
O8-P2-N4	110.4(3)	O1-C1-N2	118.5(5)
O8-P2-N6	111.2(2)	N1-C1-N2	118.0(5)
N6-P2-N4	98.5(2)	O6-C4-N6	123.4(6)
O4-P1-O3	116.5(3)	O6-C4-N5	119.2(5)
O4-P1-N3	111.0(3)	N6-C4-N5	117.4(5)
O4-P1-N1	109.5(3)	O5-C3-N4	123.5(6)
O3-P1-N3	108.5(3)	O5-C3-N5	119.4(5)
O3-P1-N1	111.7(3)	N4-C3-N5	117.0(5)
N1-P1-N3	98.2(3)	C3-N5-C4	126.9(5)
C2-N3-P1	126.7(4)	O2-C2-N3	122.2(5)
C3-N4-P2	129.7(4)	O2-C2-N2	119.4(5)
C1-N1-P1	127.9(4)	N3-C2-N2	118.3(5)

**Table S6.** Selected hydrogen-bond interactions of RPNCO.

D-H···A	d(D-H) (Å)	d(H···A) (Å)	d(D···A) (Å)
N1-H1-O3	0.880	1.935	2.815
N2-H2-O4	0.998	1.837	2.780
N3-H3-O8	0.880	2.002	2.810
N4-H4-O7	0.880	1.917	2.773
N5-H5-O8	0.880	1.984	2.856
N6-H6-O2	0.880	1.962	2.825
O9-H8-O3	1.035	1.992	2.920

## References

1. O. V. Dolomanov, L. J. Bourhis, R. J. Gildea, J. A. K. Howard and H. Puschmann, OLEX2: a complete structure solution, refinement and analysis program, *J. Appl. Crystallogr.*, 2009, **42**, 339-341.
2. G. M. Sheldrick, A short history of SHELX, *Acta Crystallogr. Sect. A*, 2008, **64**, 112-122.
3. G. M. Sheldrick, SHELXT - Integrated space-group and crystal-structure determination, *Acta Crystallogr. Sect. A*, 2015, **71**, 3-8.
4. A. L. Spek, Single-crystal structure validation with the program PLATON, *J. Appl. Crystallogr.*, 2003, **36**, 7-13.
5. B. E. Sorensen, A revised Michel-Levy interference colour chart based on first-principles calculations, *Eur. J. Mineral.*, 2013, **25**, 5-10.
6. L. L. Cao, G. Peng, W. B. Liao, T. Yan, X. F. Long and N. Ye, A microcrystal method for the measurement of birefringence, *Crystengcomm*, 2020, **22**, 1956-1961.
7. S. J. Clark, M. D. Segall, C. J. Pickard, P. J. Hasnip, M. J. Probert, K. Refson and M. C. Payne, First principles methods using CASTEP, *Zeitschrift Fur Kristallographie*, 2005, **220**, 567-570.
8. M. C. Payne, M. P. Teter, D. C. Allan, T. A. Arias and J. D. Joannopoulos, Iterative minimization techniques for ab initio total-energy calculations - molecular-dynamics and conjugate gradients, *Rev. Mod. Phys.*, 1992, **64**, 1045-1097.

9. W. Kohn and L. J. Sham, Self-consistent equations including exchange and correlation effects, *Physical Review*, 1965, **140**, 1133-1145.
10. J. P. Perdew, K. Burke and M. Ernzerhof, Generalized gradient approximation made simple, *Phys. Rev. Lett.*, 1996, **77**, 3865-3868.
11. A. M. Rappe, K. M. Rabe, E. Kaxiras and J. D. Joannopoulos, Optimized pseudopotentials, *Phys. Rev. B*, 1990, **41**, 1227-1230.
12. H. J. Monkhorst and J. D. Pack, Special points for brillouin-zone integrations, *Phys. Rev. B*, 1976, **13**, 5188-5192.
13. J. Heyd, G. E. Scuseria and M. Ernzerhof, Hybrid functionals based on a screened Coulomb potential (vol 118, pg 8207, 2003), *J. Chem. Phys.*, 2006, **124**, 1.